Near Infrared Raman Spectroscopic Study of Reactive Gliosis and the Glial Scar in Injured Rat Spinal Cords.

Tarun Saxena[a], Bin Deng[a], Eric Lewis-Clark[b], Kyle Hoellger[c], Dennis Stelzner[d], Julie Hasenwinkel[a], Joseph Chaiken[*e]
Department of Biomedical and Chemical Engineering [a], and the Department of Chemistry [e] Syracuse University, Syracuse, New York, 13244, Department of Chemistry[b], and the Department of Biomedical Engineering[c] SUNY Binghamton, Binghamton, New York, 13902, Department of Cell and Developmental Biology [d], SUNY Upstate Medical University, Syracuse, New York, 13210

ABSTRACT

Comparative Raman spectra of *ex vivo*, saline-perfused, injured and healthy rat spinal cord as well as experiments using enzymatic digestion suggest that proteoglycan over expression may be observable in injured tissue. Comparison with authentic materials *in vitro* suggest the occurrence of side reactions between products of cord digestion with chondroitinase (cABC) that produce lactones and similar species with distinct Raman features that are often not overlapped with Raman features from other chemical species. Since the glial scar is thought to be a biochemical and physical barrier to nerve regeneration, this observation suggests the possibility of using near infrared Raman spectroscopy to study disease progression and explore potential treatments *ex vivo* and if potential treatments can be designed, perhaps to monitor potential remedial treatments within the spinal cord *in vivo*.

Keywords: Spinal cord injury, glial scar, Raman, chondroitin sulfate proteoglycans, chondroitinase ABC

1. INTRODUCTION

Spinal cord injury (SCI) is a debilitating condition leading to paralysis and is currently affecting more than a million Americans with annual healthcare costs exceeding 40 billion dollars[1, 2]. Intensive research efforts are ongoing to understand and treat SCI. Currently, histology and immunohistochemistry are gold standards for obtaining qualitative and quantitative information about cellular and biochemical components of tissues. However, these are exclusively *ex vivo* techniques, requiring preprocessing of tissues and altering their native state. The main goal of this research is to explore the possible use of Raman spectroscopy (RS) in assessing the chemical and physical state of relevant tissues in their native state. Near infrared (NIR) Raman spectroscopy (RS) presents the possibility of minimally or possibly non-invasive monitoring of SCI progression and possibly treatment regimens *in vivo*. We present spectra of rat spinal cords, healthy and injured, at different stages of glial scar formation and development. In connection with the possibility of monitoring treatment regimes, and in attempting to understand to some degree the evolution of the spectra with the development of the SCI, we present *in vitro* data involving enzymatic digestion of authentic samples of one extracellular matrix (ECM) material for comparison.

While there are different types of SCI, and we present data concerning one type, there are some common empirical observations that would be helpful to review in order to appreciate the rationale for this research approach. After SCI, a scar forms at the site of the injury that is known as the glial scar. Regenerating axons often retract or stop extending once they encounter the glial scar. The glial scar contains various cell types and the extracellular matrix (ECM) produced by those cells. This ECM consists of both inhibitory and growth permissive molecules. The consequences of SCI are quite complex but at the outset we note that spontaneous Raman spectroscopy is generally not a technique capable of detecting materials in mixtures at less than the part per thousand level of abundance. This has the effect of simplifying the actual data in the sense that observable Raman spectral features *in vivo* are dominated materials that are present in relative bulk and/or have repeating units that cause spectral features to pile-up in certain spectral regions, e.g. amide I or CH_2 deformation. Any small molecule analyte present in less than 1 millimolar concentration is not likely to be observed. The

* jchaiken@syr.edu, phone 315 443 4285

Biomedical Vibrational Spectroscopy IV: Advances in Research and Industry, edited by Anita Mahadevan-Jansen, Wolfgang Petrich, Proc. of SPIE Vol. 7560, 75600I · © 2010 SPIE · CCC code: 1605-7422/10/$18 · doi: 10.1117/12.846897

exception is water with its very small Raman crossection but roughly 55.5 M concentration such that it and many other materials together contribute to a smooth low level baseline.

Following SCI, the cascade of events can be divided into three phases: the primary or immediate phase, the secondary or acute phase, and the chronic phase [3]. In the immediate phase, due to the mechanical insult to the spinal cord at the lesion site, there is a complex cascade of primary events followed by secondary effects orchestrated by the host's immune system. There is immediate cell death of neurons and glial cells such as oligodendrocytes, astrocytes, and endothelial cells due to the mechanical trauma locally at the site of injury and the surrounding tissue. Increased neuronal and astrocytic cell death and invasion of the inflammatory cells such as macrophages, and monocytes, causes an increase in excitatory molecules such as glutamate and peroxides. Further, when astrocytes are subjected to trauma, they become reactive, which causes them to proliferate and increase the production of intermediate filaments made up of glial fibrillary acidic protein.

The secondary phase lasts for hours to a few days. During this period the astrocytes begin to migrate out of the lesion center as well as to produce molecules such as proteoglycans and laminin in the extracellular space. In the chronic phase of injury there is continued necrosis and also demyelination in the white matter due to apoptotic oligodendrocytic death. Reactive astrocytes continue to invade the region surrounding the lesion center and begin to wall off this region, forming what is classically known as the glial scar.

The glial scar walls off the site of injury and consists mainly of reactive astrocytes and the chondroitin sulfate proteoglycans (CSPGs) secreted by these astrocytes. Further, due to meningeal breakdown in the case of a hemisection injury, there is an infiltration of fibroblasts into the lesion and these fibroblasts produce collagen [4]. Apparently the presence of this glial scar and the lesion core that it subsumes is inhibitory to axonal regeneration. The glial scar has been hypothesized to be a physical and a biochemical barrier to axonal regeneration [4-6].

Based on this hypothesis various researchers have proposed that if the effectiveness of the glial scar as a biochemical and physical barrier could be degraded, then perhaps with the addition of appropriate growth factors, the tissues could be induced to repair themselves by revascularization and axonal regeneration [7-9]. The desire to degrade the barrier inspired the suggestion to use chondroitinase (cABC), a bacterial enzyme produced by the bacteria *proteus vulgaris* to assist the process. cABC is not produced by the human body and so would need to be introduced by external means. It is thought that that the CSPGs act as repellents to these bacteria and they evolved to produce cABC in order to invade the wound better.

The objective of this work is to develop the use of RS as a reliable method to identify temporally, various biochemical components of the glial scar in its native physiological state without homogenization, extraction, or the use of dyes, or contrast enhancing labels. All the materials that are produced in reaction to SCI are composed of the usual proteins, lipids and carbohydrates. The linkages between them are the things that vary in the Raman spectra of healthy versus injured cord, in addition to the internal modes of these constituents that are well known from the last 30 years of biological spectroscopy [10]. In addition, just as there are post transcription, enzymatic and non-enzymatic, modifications of proteins in healthy cells and tissues, we expect such processes to also occur in injured spinal cord but involving the materials and environment specific to injured cord. It is our hope that successful culmination of this work will provide a sound basis for future *in vivo* work. The animal model chosen for this work is the rat, with the injury model being a lateral hemisection. The glial scar is evaluated spectroscopically at 4 days; 2 weeks and 8 weeks post injury. We present data showing *in vitro* Raman spectra of cABC acting on authentic chondroitin sulfate that we subsequently compare with the spinal cord spectra.

2. METHODOLGY

2.1 Hemisection surgery

The Institutional Animal Care and Use Committee (IACUC) at Syracuse University approved this study. The rat was anesthetized with Ketamine and Xylazine (80mg/kg and 10 mg/kg respectively) and the body temperature maintained using a heat lamp. Aseptic surgery was performed using the following technique. The skin over the upper thoracic area was shaved and cleaned with a Betadyne solution. The skin was incised, and then the connective and muscle tissue were bluntly dissected to expose T9. A T9 laminectomy was completed, taking care not to damage the spinal cord during the dorsal lamina removal. A lateral hemisection was performed at T9; initially a surgical needle punctured the spinal cord dorsoventrally at the midline avoiding the dorsal spinal artery; angled microscissors were then used to cut the right half

of the spinal cord followed by an angled needle scraping the vertebrae ventrally and laterally surrounding the lesion to ensure completeness of the hemisection. Finally, the lesion was closed in layers with individual sutures. A schematic of the hemisection surgery is shown in Figure 1.

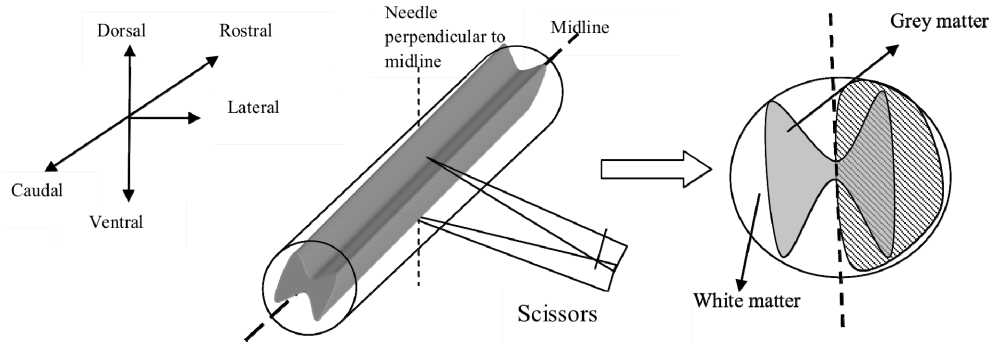

Figure 1 schematic of the hemisection injury model. The cord is oriented in the rostro-caudal direction. A needle is inserted at the midline dorso-ventrally and angled microscissors are then used to transect one half the cord, latero-medially. The resulting injury is shown in a transverse section. The shaded portion is the injured side and the non-shaded portion is the contralateral uninjured side.

The animals were then sacrificed at various time points post injury. Injured spinal cords were excised using a posterior approach. Euthanasia, by perfusion of the rats with physiological phosphate buffered saline (PBS), was followed by a laminectomy between the first cervical vertebra (C1) and the 4th lumbar vertebra (L4). The nerve roots were carefully severed and the spinal cord was cut at levels C1 and L4, then carefully removed and placed in a bath of isotonic phosphate buffered saline. No attempt was made to remove the Dura mater. The cords were then stored in a refrigerator at 4^0C until testing. All testing was performed within 4 hours of excision of the spinal cords. A total of 21 animals were used. Six animals were used for each time point post injury (n=18 total) and three animals were used as controls (n= 3). The control animals did not receive any injury and the cords excised from them were termed as healthy cords.

2.2 Raman spectroscopy

A schematic diagram of the instrumentation is shown in Figure 2. The laser wavelength was 785 nm (Process Instruments, Salt Lake City, Utah) and spectra were collected in backscatter mode. The laser power at the sample was 450 mW and the spot size was 300 μm determined using Zap-it paper.

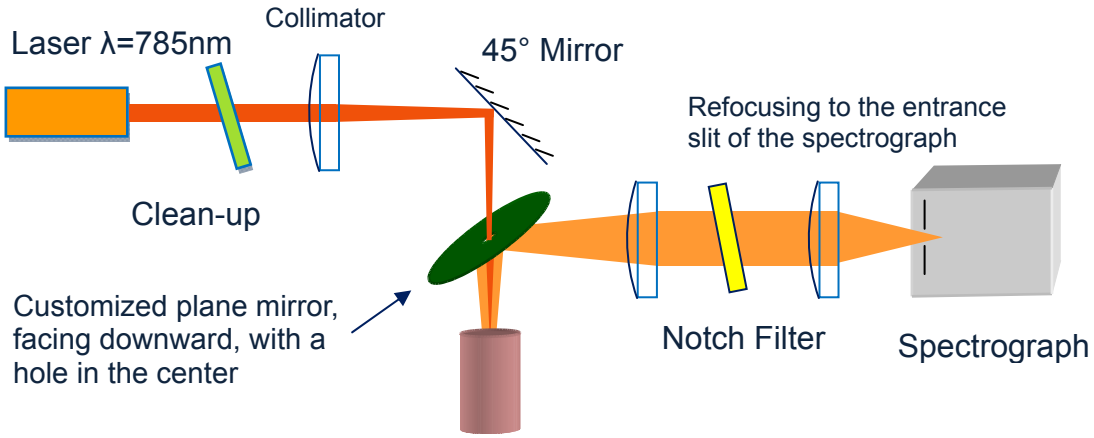

Figure 2. Schematic diagram of *in vitro* Raman apparatus.

For *in vitro* experimentation a fused silica cuvette is employed for liquid samples and a Roper Scientific/PAR CCD camera detects the light after dispersion by a Kaiser f/1.4 Holospec spectrograph. The chondroitinase and the chondroitin sulfate were obtained from Sigma Aldrich and both were used as received.

The spinal cord was oriented similar to it's orientation *in-vivo* with the dorsal side facing up. The cord was placed in a specially designed quartz holder that is placed on a 3-D staged controlled with micrometers and care was taken to keep the spinal cord hydrated with PBS during the course of an experiment. The spectra do change in a systematic manner if allowed to dry out. As shown in Figure 3, spectra were obtained in the region circumscribing the scar (10 spectra, 5 minutes each), focusing on the scar (12 spectra, 5 minutes each), and on a healthy region of the cord away from the injury site (3 spectra, 5 minutes each). All experiments were done at room temperature.

Using Matlab® custom written routines spectra were cropped in the fingerprint region (400 cm^{-1}- 1800 cm^{-1}) and were corrected for background fluorescence using an arbitrary but unbiased 101-point moving window-averaging scheme [11]. The background corrected spectra were smoothed using a 7-point moving window algorithm and when noted, mean centered and divided by the standard deviation, i.e. the standard normal variate [SNV] transform.

3. DATA AND RESULTS

3.1 Raw data of healthy and injured spinal cords and variation in fluorescence

Figure 3 shows the unprocessed data obtained from a single location on a single spinal cord at certain times after spinal cord injury. Along side is shown a representative time course for the integrated fluorescence on a single location of a particular cord for successive 5-minute CCD acquisitions. Figure 3a is representative of healthy cord, and Figures 3b, 3c and 3d of spinal cords 4 days, 2 weeks, and 8 weeks post injury respectively. It can be seen that there is background fluorescence but the Raman peaks are evident and that the relative magnitude of these peaks is similar (for each disease condition), irrespective of the fluorescence, although 8 of 10 locations on the healthy cord produced data within ±3% of the average. The other 2 locations produced a large bivariate deviation from average. We observe that fluorescence of spinal cord bleaches with extended irradiation at a single location. For *most* of the data, the fluorescence variation with time is commensurate with the variation observed by sampling spectra from different but apparently identical locations on the same cord.

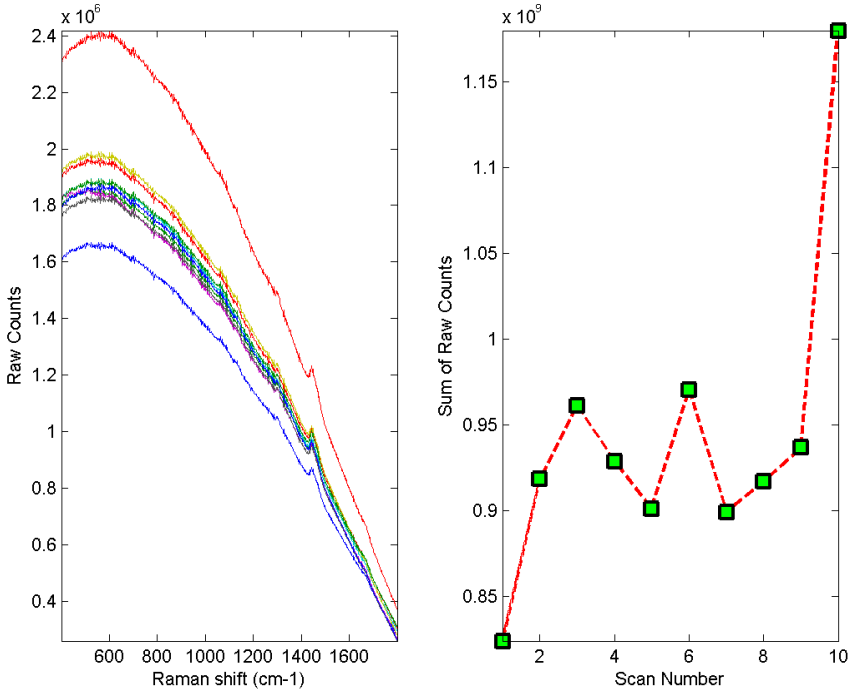

Figure 3a left: collected spectra at different locations on a healthy cord, right: integrated fluorescence as a function of position.

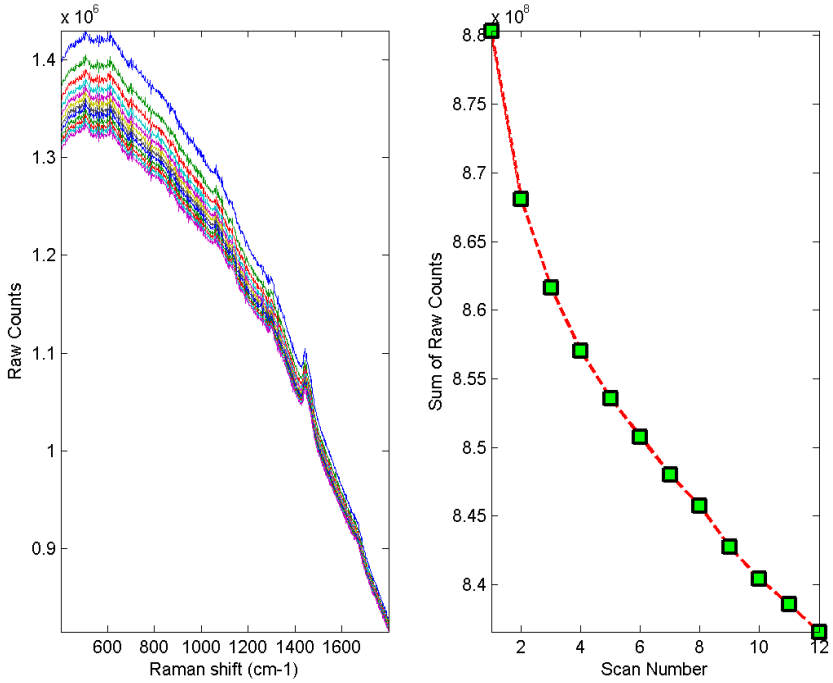

Figure 3b left: collected spectra at the same location as a function of time, right: integrated fluorescence as a function of time (5 min/scan number) for a four-day post injury spinal cord

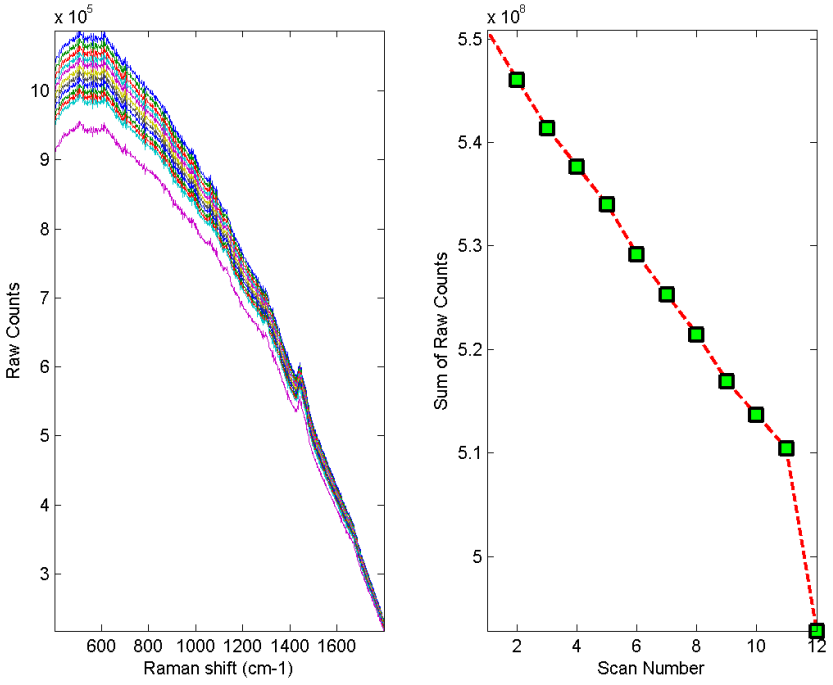

Figure 3c left: collected spectra at the same location as a function of time, right: integrated fluorescence as a function of time (5 min/scan number) for a 2-week post injury spinal cord.

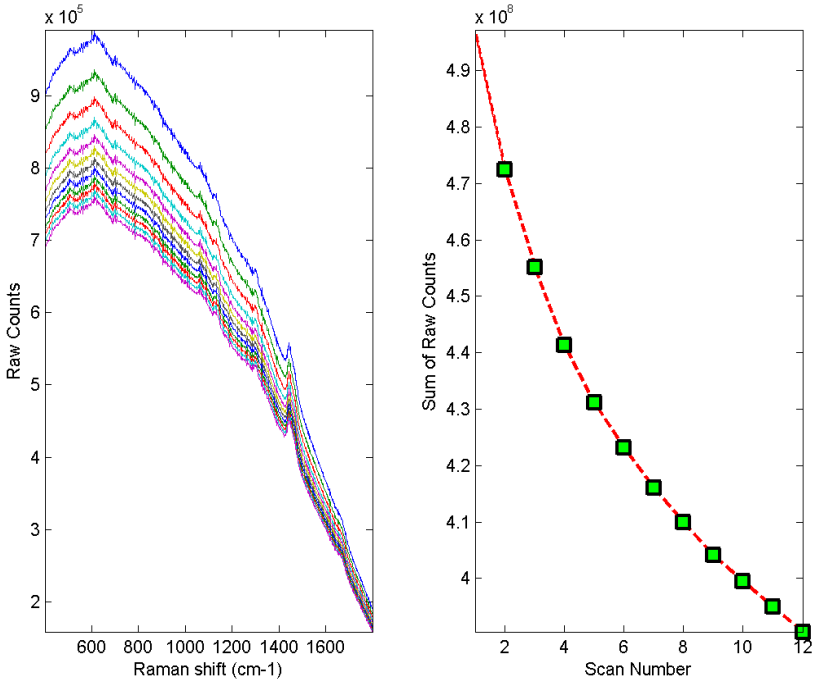

Figure 3d left: collected spectra at the same location as a function of time, right: integrated fluorescence as a function of time (5 min/scan number) for a 2-week post injury spinal cord.

Further, it is also clear that the spectra contain Raman features that are relatively constant with respect to the fluorescence, indicating that the photobleaching or the location did not affect the relative Raman spectral features.

In order to see this more clearly, Figure 4 shows the average of all the spectra taken either on healthy tissue or different locations within the SCI zone for each injured cord at each time (total number of rats per group as in methodology section). The fluorescence for the healthy cord is substantially larger and spectrally narrower than for any of the injured rats. The fluorescence of the injured cords decreased monotonically with time post injury.

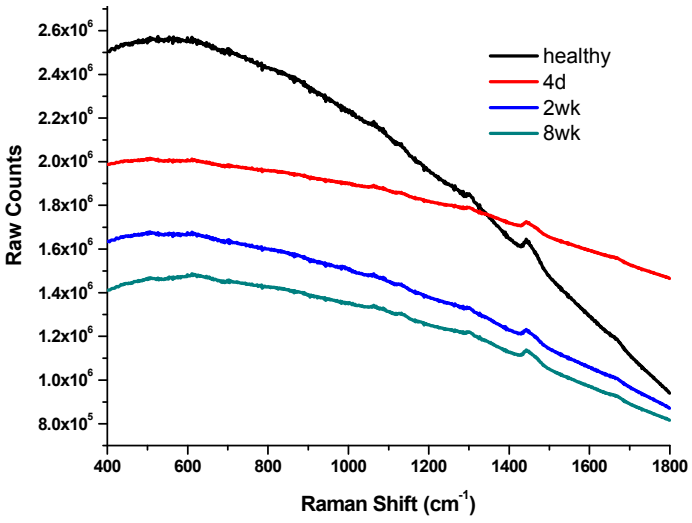

Figure 4 the average of all the spectra taken either on healthy tissue or different locations within the SCI zone for each injured cord at each time point. The standard deviations about the average spectra are ± 5%.

3.2 Raman spectra of healthy and injured spinal cord at different times post injury

Applying the 101-7 smoothing baseline correction algorithm and the SNV transform to the data in figure 4 produces the Raman spectra shown in Figure 5. Despite being the averages over many rats very systematic variation can be perceived. Certain features such as the 1450 cm^{-1} CH_2 deformation mode and the 1760 cm^{-1} amide I modes are very prominent in all the spectra and overlaid do not appear to vary much at all with post injury time. In order to see the variation we produce difference spectra and so using the healthy cord as reference, Figure 6 reveals very systematic variations that are often, but not always monotonic.

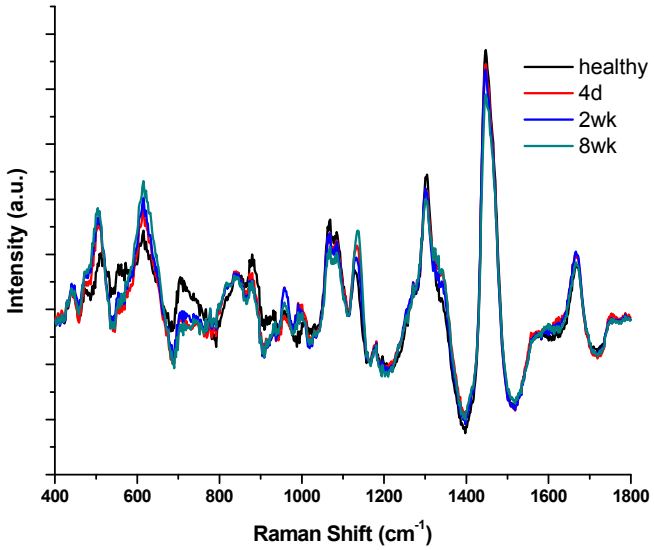

Figure 5 Overlaid baseline corrected average spectra of all rat spinal cords at different times post-injury.

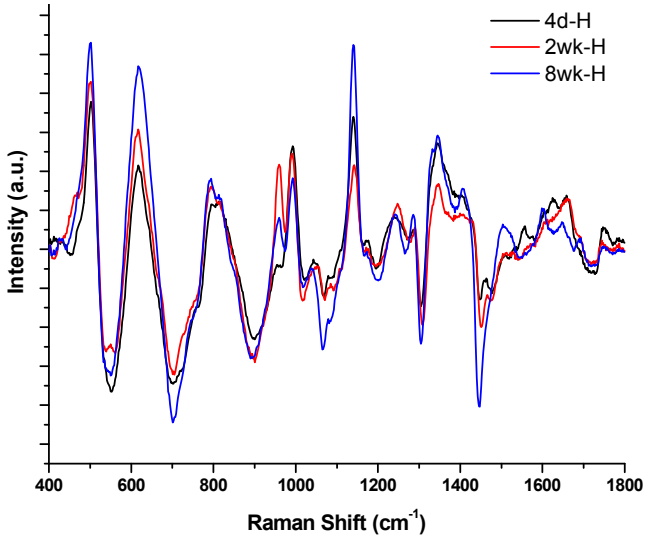

Figure 6 Difference spectra obtained from data in Figure 5

We observe in Figure 6 that relative to the healthy spinal cord tissue, the tissue in and around injured spinal cord monotonically loses materials that produce the 1450 cm^{-1} and 1000 cm^{-1} features but monotonically gains the materials associated with the features at 500 and 600 cm^{-1}. Other features, notably near 960 cm^{-1} and above 1500 cm^{-1}, have more complex behavior with time post injury.

In terms of a possibly comparable *in vitro* system, Figure 7 shows the room temperature time evolution of the water subtracted, baseline corrected Raman spectrum of a mixture of cABC and chondroitin-6 sulfate in phosphate buffered saline. Chondroitin-6 sulfate consists of a long polysaccharide chain with free carboxylic acid groups, sulfate groups and methyl amide groups as well. The spectrum of the un-digested material displays well-known features at 600 cm^{-1} and below corresponding to ring vibrations of the individual saccharides, and the 1067 cm^{-1} corresponding to sulfate. In addition we observe overlapping Raman features near the anomeric carbon linkage mode near 800-900 cm^{-1} as well as a variety of features about 1600 cm^{-1} corresponding to the amide linkages and carboxylic acid carbonyl localized modes.

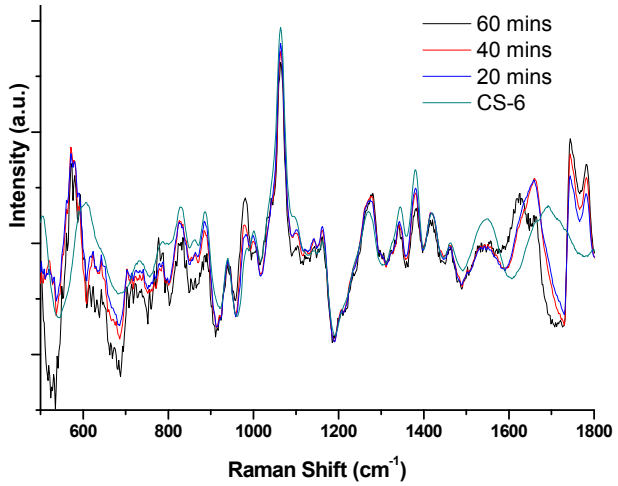

Figure 7 time course of cABC digestion of chondroitin 6-sulfate in PBS at room temperature.

4. DISCUSSION

There are clearly some systematic changes in the spectra that bear discussion in the context of the known development of the glial scar that was reviewed earlier and the known strengths and limitations of spontaneous Raman spectroscopy. The results also suggest some improvements in experimental technique going forward and this will be discussed as well. We shall discuss these results in the order they were presented above in the context of possibly monitoring treatment regimes, and in attempting to understand to some degree the evolution of the spectra with the development of the SCI.

First, we note that the observed fluorescence can vary by as much as 15% depending on the exact location of probing, even in healthy tissue. Since 80% of the data is quite well behaved, ±3%, and fluorescence cannot be produced unless the incident light penetrates the surface, we suggest that much of the observed variation in *absolute* fluorescence in 80% of the sampled locations results from small surface angle changes and this is generally what should be expected in *in vivo* applications. We suggest that the observed wild variation in *absolute* fluorescence in the 20% sampled locations results from some inhomogeneity introduced by the process of obtaining and handling an *ex vivo* sample, e.g. a nick or bubble or speck of dried blood or other debris, and not to the *general existence* of some form of optical inhomogeneity on the scale of the laser diameter on the surface of spinal cord generally. Included in this effect would be the fact that the efficiency of observation of emission from beneath the surface also depends on the angle of incidence and the exact depth of a particular fluorophore[11, 12]. Thus the overall consistency of the data suggests that the procedure of comparing Raman spectra that have been treated with the SNV transform should reasonably accurately reflect relative changes in the composition of the probed tissues.

The absolute fluorescence is important in the context of *ex vivo* and *in vivo* studies if there is a desire to possibly associate the fluorescence with the volume of the probed region. In order to quantify Raman spectra for biomedical samples in the past we have normalized Raman spectra to the underlying fluorescence with some success [13] but this approach may be problematic for *in vivo* SCI applications if we choose to be completely non-physical contact in our methods. In this regard we note that we have previously used Brewster's Angle as a starting point, ≈53º for most tissue-air interfaces, because it maximizes the transmission of light into the sample thereby maximizing the resultant spectroscopic signals. The variation of the Fresnel coefficients with incident angle are also just as flat there as for around 0º angle of incidence. Moreover this geometry with free space coupling minimizes the production of spurious Raman and fluorescence of the optical components themselves [14]. It is certainly conceivable that in practice for *in vivo* applications, monitoring the specular reflection from the cord surface could potentially provide a completely non-contact feedback mechanism for initially setting and then maintaining an optimal or at least consistent angle of incidence while probing the cord. We suspect that approach might be easier to accomplish in non-normal incidence and overall this might offer a more consistent basis for comparing absolute fluorescence from location to location and at the same location over the passing of time.

Given the observed site-to-site variation for the same cord, the variation of the absolute fluorescence with time post injury, averaged over multiple rats and locations, is significant. It is quite possible that normal homeostasis simply produces more of some fluorescent species per unit volume than injured tissue and less of at least one other fluorescent species. In this respect we observe that the variation is monotonic with time, which seems to support this simple interpretation although the ratio of the two components seems to be constant within all the injured cord data and within all the healthy cord data. The wider spectral emission suggests that there is apparently another significant fluorophore in injured cord that is not present in healthy cord. We note that a likely *new* significant fluorophore is trapped dried blood that would presumably contain methemoglobin and should have a fluorescence that is shifted from that of other hemoglobins since the absorption spectrum shifted.

These observations could be connected to the empirical observation that at some point after the initial insult the tissues generally attempt to revascularize [15]. Each rat's entire circulatory system was thoroughly perfused with PBS before the cord was removed in an effort to remove all traces of the blood, particularly hemoglobin, from the probed volume. But given the strong fluorescence quantum yield of all porphyrins, we never expected to succeed in completely removing all heme-based emission. Since hemoglobin is generally the strongest fluorophore in any probed volume *in vivo*, we hypothesize that the total fluorescence could be a function of the degree to which a probed volume of the SCI has been revascularized. Immediately, i.e. within two days after the SCI there is no repair yet to the local vascular system and the perfusion has to wash away blood from the initial insult. By two weeks time new vessels have begun to appear and the possibility of some new blood being in the probed region is greater but the perhaps the probability of trapping erythrocytes is a function of the amount of new blood being present, leading to more expected net fluorescence on average at that time point with essentially the same ratio of good heme emission to methemoglobin emission. Since the cords were intentionally damaged so that they could not recover on their own, the attempt to revascularize must fail, all new vessels must atrophy, decreasing the transport of new blood into the region, so that at eight weeks post SCI there would be less blood to be perfused away and the fluorescence should continue to decrease.

It is also true that there was no unequivocal evidence from the data shown in this paper to suggest that the fluorescence from the injured cords must originate from a blood borne fluorophore. Since only the gray matter is vascularized and in spinal cord the gray matter is covered by the more highly scattering but unvascularized white matter, the choice of 785 nm excitation wavelength may have precluded sufficiently efficient depth penetration to produce sufficient observable fluorescence. Preliminary experiments with 830 nm excitation suggest that fluorescence originating with subsurface grey matter, i.e. blood, can be reliably detected and we hope to conduct another rat study to ascertain whether revascularization can in fact be observed noninvasively *ex vivo* using 830 nm excitation.

In this same connection we can see that some of the Raman features actually do have a non-monotonic time course post SCI. In the range of 960-970 cm^{-1} and near 1560 cm^{-1} Raman shift we see a decrease-increase-decrease time course as might correlate with revascularization. Actual resonance and spontaneous Raman features for hemoglobin are known [16] in these regions but these would then be expected to correlate with the fluorescence behavior if the *majority* of the observed fluorescence can in fact be associated with incompletely removed blood by the PBS perfusion. If this is not the case, i.e. there are other more productive fluorophores than hemoglobin in the probed volume, either by having much greater concentration or quantum yield, then it is possible that we could observe revascularization using Raman features and not be able to observe a correlated change in observed fluorescence. We cannot settle this issue either way with only

the results of the present experiments but a more complete picture could be provided by planned histological studies of the cord tissues at the same time points post injury in addition to the planned 830 nm experiments.

Of the Raman features that apparently change monotonically post injury there would appear to be two types. The decrease in 1450 cm^{-1} CH_2 deformation Raman activity may correspond to demyelination of the axons whereas the large increase in Raman intensity below 600 cm^{-1} could be associated with increased CSPG expression as is known to occur empirically. The relevant structure of the ECM is shown below in Figure 9. The need to produce extraordinary amounts of a particular material with many repeating subunits in order to be observable by Raman is certainly met in this case. But perhaps more interesting is the activity about 1600 cm^{-1} in which we see a range of new features appear extending to rather high Raman shifts, i.e. exceeding 1700 cm^{-1}.

We propose in this case that the conditions in the injured cord are conducive to acid catalyzed hydrolysis of the polysaccharide chains. This would be expected to be a slower process but in essence with the same reaction products as the cABC digestion. The local medium would be expected to be mildly but increasingly acidic because at death the blood and tissues becomes hypoxic and therefore acidic. Although PBS was employed in the circulatory system, the blood pH is maintained with the bicarb based buffer system and this shuts down completely in minutes after death so that the serviced tissues and therefore the site of the ECM are immediately hypoxic and become increasingly acidic unless the tissues become revascularized which takes days and weeks *in vivo*. Although the acid catalyzed reactions are expected to be slow we note that the observed changes take place over weeks in injured cord but in less than an hour in the cABC catalyzed reaction. In the case of cord post injury in vivo, monosaccharides and perhaps even multi-saccharides would be produced directly but in the cABC digestion only disaccharides are first produced which we suggest are then hydrolyzed *in situ* to produce monosaccharides. Taking this one step further we propose that the monosaccharides, being in equilibrium with their linear chain forms, produce lactones as more monosaccharides are produced. Because the lactones have a rather high carbonyl Raman shift, i.e. about 1750 cm^{-1}, they are more easily observed than some other species due to lack of spectral congestion. The entire scheme is laid out below in Figure 10.

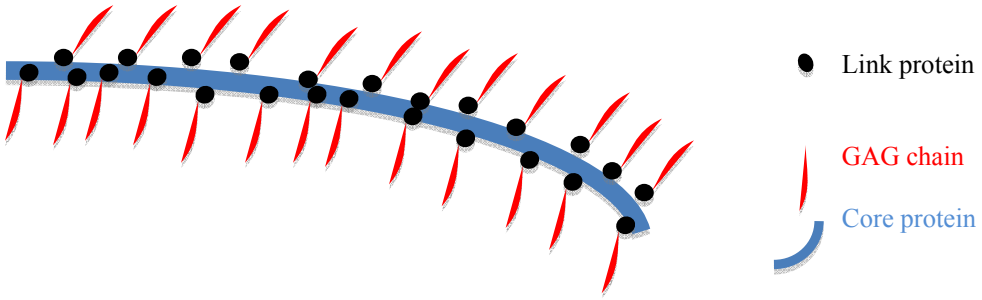

Figure 9 schematic representation of ECM showing CSPGs (proteoglycans are on the GAG chains) and organization of various components.

As can be seen in Figure 10 there are functional groups, i.e. carboxylic acids, hydroxyls and amides that would be expected to interact in various ways, including isomerization after formation of the straight chain forms, but because they all participate in carbonyl chemistry, all would be expected to produce a variation in the Raman activity at above1670 cm^{-1}, as is observed. A question mark is included to indicate that the chemistry could be quite complicated here but we suggest that the amide group could hydrolyze and then react with other carboxylic acid groups on other saccharides to produce a succession of structurally similar products in relatively large quantity due to the SCI induced over expression of the CSPGs. Over expressed by the astrocytes, the CSGPs are the primary reactant in this overall scheme.

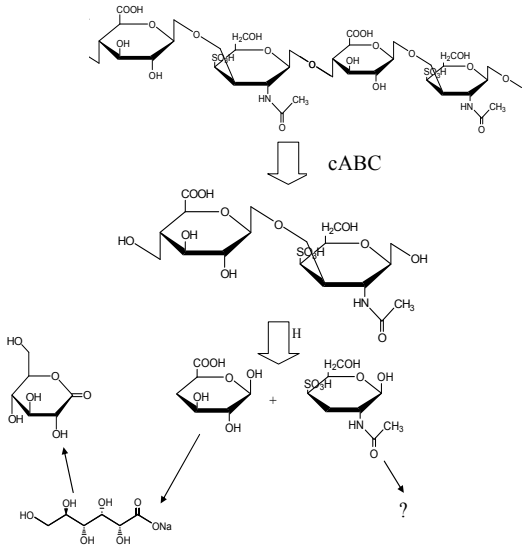

Figure 10 reaction scheme representing the action of cABC on chondroitin sulfate and subsequent acid catalyzed hydrolysis and rearrangement of products.

5. CONCLUSIONS

We believe the NIR Raman spectra presented in this paper strongly support the proposition that SCI can be monitored noninvasively and quite possibly *in vivo*. There is considerable variation between the Raman spectra of healthy spinal cord and injured cord and the differences, and their time course post injury, are reasonably well correlated with known empirical tissue and metabolic changes that accompany SCI. Since the action of cABC on authentic chondroitin-6-sulfate can be easily discerned and followed, it seems quite reasonable to suggest that if cABC were used to "soften" or perhaps even inhibit the initial formation of the physical and biochemical barrier presented by the glial scar, the progression of that treatment could be followed using NIR Raman spectroscopy. Particularly exciting in this respect is the possible formation of a lactone as a natural course of the cascade of expected side reactions *in vivo* since the lactone carbonyl stretch occurs in a region that is unlikely to be obscured by spectral congestion despite the very complicated mixture presented by an evolving *in vivo* system. Thus NIR Raman offers some very exciting possibilities with respect to diagnosing, monitoring and treating SCI *in vivo* in the future.

ACKNOWLEDGEMENTS

A fellowship from the Syracuse Biomaterials Institute supported Tarun Saxena and LighTouch Medical, Inc. supported Bin Deng. The authors appreciate the continued discussions with Dr. George Shaheen of LighTouch Medical. Machine shop fabrication was by Lou Buda, Charlie Brown, Phil Arnold and Les Schmutzler. Sally Prasch at the glass shop fabricated the cuvettes. Assistance with the design and optimization of our optical system by Rebecca J. Bussjager is gratefully acknowledged. NSF funding of the Syracuse University REU program made the participation of Eric Lewis-Clark and Kyle Hoellger possible.

REFERENCES

[1] http://www.spinalcord.uab.edu/show.asp?durki=116979.
[2] http://www.christopherreeve.org/site/c.geIMLPOpGjF/b.1402847/k.EE60/SCI_Facts.htm.
[3] Hagg, T. & Oudega, M. Degenerative and spontaneous regenerative processes after spinal cord injury. J. Neurotrauma 23, 264-280 (2006).
[4] Silver, J. & Miller, J. H. Regeneration beyond the glial scar. Nat. Rev. Neurosci. 5, 146-156 (2004).
[5] Yu, X. & Bellamkonda, R. V. Dorsal root ganglia neurite extension is inhibited by mechanical and chondroitin sulfate-rich interfaces. J. Neurosci. Res. 66, 303-310 (2001).
[6] Ramón y Cajal, S. in Degeneration and regeneration of the nervous system (Oxford University Press, London, 1928).
[7] Dodla, M. C. & Bellamkonda, R. V. Differences between the effect of anisotropic and isotropic laminin and nerve growth factor presenting scaffolds on nerve regeneration across long peripheral nerve gaps. Biomaterials 29, 33-46 (2008).
[8] Fitch, M. T. & Silver, J. CNS injury, glial scars, and inflammation: Inhibitory extracellular matrices and regeneration failure. Exp. Neurol. 209, 294-301 (2008).
[9] Bradbury, E. J. et al. Chondroitinase ABC promotes functional recovery after spinal cord injury. Nature 416, 636-640 (2002).
[10] Tu, A. T. in Raman spectroscopy in biology: principles and applications (Wiley, New York, 1982).
[11] Chaiken, J. & Goodisman, J. On probing human fingertips *in vivo* using near infrared light: model calculations. Submitted 12-13-09.
[12] Matousek, P. et al. Numerical simulations of subsurface probing in diffusely scattering media using spatially offset Raman spectroscopy. Appl. Spectrosc. 59, 1485-1492 (2005).
[13] Chaiken, J. et al. Effect of hemoglobin concentration variation on the accuracy and precision of glucose analysis using tissue modulated, noninvasive, *in vivo* Raman spectroscopy of human blood: a small clinical study. J. Biomed. Opt. 10, 031111 (2005).
[14] Chaiken, J. et al. Noninvasive, in-vivo, tissue modulated near infrared vibrational spectroscopic study of mobile and static tissues: blood chemistry. *Proc. SPIE*, Vol. 3918, 135-143 (2000)
[15] Weidner, N., Grill, R. J. & Tuszynski, M. H. Elimination of basal lamina and the collagen 'scar' after spinal cord injury fails to augment corticospinal tract regeneration. Exp. Neurol. 160, 40-50 (1999).
[16] Franzen, S., Wallace-Williams, S. E. & Shreve, A. P. Heme charge-transfer band III is vibronically coupled to the Soret band. J. Am. Chem. Soc. 124, 7146-7155 (2002).